

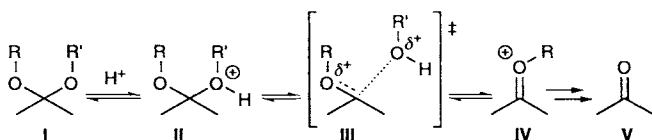
Catalytic Antibodies as Probes of Evolution: Modeling of a Primordial Glycosidase**

Doron Shabat, Subhash C. Sinha,* Jean-Louis Reymond,* and Ehud Keinan*

Enzymes achieve remarkable catalytic efficiency by several effects operating in concert. This is the result of evolution and natural selection over eons. One might wonder how primordial enzymes became catalytically active in the first place. To answer such a question it is important to know which of the effects operating in a modern enzyme is capable of triggering catalysis independently of the others. Catalytic antibodies,^[1] which are designed by the experimenter, offer a unique opportunity to study such issues and to examine experimentally various hypotheses about primordial enzymes. It is much easier to dissect the individual parameters of catalysis in catalytic antibodies than in highly evolved enzymes in which all these parameters operate together. Indeed, Schultz et al.'s fundamental structural studies provide much insight into the evolution of catalytic capabilities in proteins.^[2]

Along these lines and owing to the importance of carbohydrates in the early stages of evolution, the emergence of glycosidase activity is of particular interest. Herein we report on an antibody-catalyzed hydrolysis of unactivated cyclic ketals, a reaction that is closely related to the cleavage of the glycosidic bond.^[3] These catalytic antibodies may therefore be considered as mechanistic analogs of the glycosidase enzymes. We show here that general acid catalysis and/or strain effects, which are of central importance in the activity of modern glycosidases,^[4] have only minor significance in these catalytic antibodies. Conversely, simple charge complementarity proves to be the major factor in determining their catalytic activity.

Hydrolysis of ketal **I** involves protonation at one of the oxygen atoms, followed by heterolysis of a C–O bond to generate the intermediate ion **IV** and ultimately the carbonyl compound **V** (Scheme 1). In the case of ketals and acetals with an activated

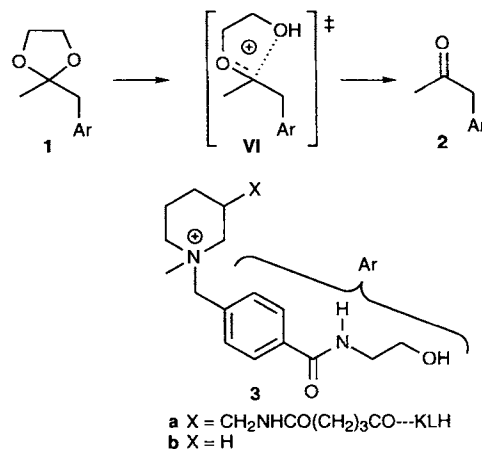


Scheme 1. General mechanism of ketal hydrolysis under acidic conditions.

leaving group (e.g. $R' = \text{aryl}$), the first step is the rate-limiting one, and their hydrolysis can be catalyzed by weak acids (general acid catalysis).^[5,6] In contrast, with unactivated ketals (e.g. $R' = \text{alkyl}$)^[7] the O-protonated species **II** is a relatively stable intermediate formed in a preequilibrium. In such cases cleavage

of the C–O bond (via transition state **III**) is the rate-limiting step. Therefore, the hydrolysis of unactivated ketals or acetals is not catalyzed by weak acids and depends only on the pH (specific acid catalysis). This reactivity pattern, which also applies for the hydrolysis of glycosidic bonds, poses a particular challenge for the design of a biocatalyst since the presence of a weak acid alone is not sufficient to promote the reaction.

Dioxolane **1**^[8] is hydrolyzed in aqueous acidic medium to give ketone **2** and ethylene glycol. Although the hydrolysis rate is pH-dependent, it is totally indifferent to the buffer type and concentration. The observed inverse solvent isotope effect ($k_H/k_D = 0.4$) confirms that the reaction is specific acid catalyzed; the rate-limiting cleavage of the C–O bond of the protonated intermediate **II** leads to the intermediate **IV**. This step involves expansion of the protonated dioxolane ring, during which the positive charge moves from the leaving oxygen atom to the remaining one. We reasoned that the piperidinium ion **3** would be an accurate analog of transition state **VI** (Scheme 2). The positively charged nitrogen center in **3** mimics the emerging ion **IV**, and the six-membered piperidinium ring mimics the expanded five-membered ring of **VI**.



Scheme 2. Transition state **VI** and transition state analog **3** for the hydrolysis of ketal **1** to ketone **2**. KLH = Keyhole Limpet H aemocyanin (carrier protein).

A series of 46 monoclonal antibodies directed against **3a**^[6a] were assayed for catalysis of the hydrolysis of **1**. Two of them, antibody 14D9 and antibody 20B11,^[9] catalyzed the reaction. In both cases catalysis followed Michaelis–Menten kinetics (Fig. 1) and was totally inhibited by the haptin (**3b**), indicating that the catalytic reactions take place in the combining sites of these antibodies.^[10]

In most of the glycosidase enzymes, shape complementarity to the transition state plays a key role in catalysis by inducing productive strain in the substrate.^[11] We attempted to obtain similar, shape-selective recognition of the inflated dioxolane ring in the transition state **VI** by using a six-membered ring transition state analog in eliciting the antibodies. To appreciate the effect of this shape complementarity on catalysis by our antibodies we studied the six- and seven-membered ring ketal analogs of substrate **1**: dioxane **4** and dioxepane **5**.

Both antibody 14D9 and antibody 20B11 catalyzed hydrolysis of dioxane **4**. However, in comparison to the hydrolysis of **1**, catalytic efficiency was reduced, in terms of both rate enhancement ($k_{\text{cat}}/k_{\text{uncat}}$ is decreased 2.6-fold with 14D9 and 8.2-fold

[*] Dr. S. C. Sinha, Dr. J.-L. Reymond, Prof. E. Keinan
Department of Molecular Biology and
the Skaggs Institute for Chemical Biology
The Scripps Research Institute
10550 N. Torrey Pines Road, La Jolla, CA 92037 (USA)
Fax: Int. code + (619) 784-7313

Prof. E. Keinan, D. Shabat
Department of Chemistry, Technion - Israel Institute of Technology
Technion City, Haifa 32000 (Israel)

[**] J.-L. R. thanks the U. S. National Institutes of Health (GM 49736) for funding.
E. K. thanks the US–Israel Binational Science Foundation and PharMore
Biotechnologies Ltd. for financial support.

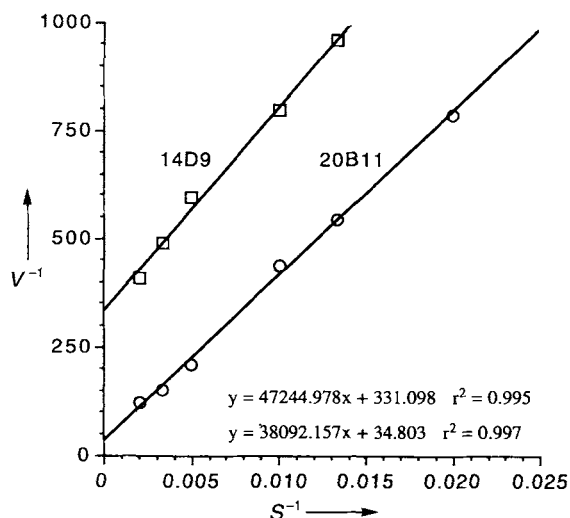


Fig. 1. Lineweaver-Burk plot of antibody-catalyzed hydrolysis of ketal **1** with antibodies 14D9 (squares) and 20B11 (circles). For the reaction conditions see ref. [10]. V = hydrolysis velocity ($\mu\text{M h}^{-1}$), S = substrate concentration (μM).

with 20B11) and transition state binding (K_{TS} is increased 4.5-fold with 14D9 and 2.9-fold with 20B11) (Table 1). This trend continued further with the seven-membered substrate **5** with a further decrease in $k_{\text{cat}}/k_{\text{uncat}}$ and increase in K_{TS} relative to the hydrolysis of **1** ($k_{\text{cat}}/k_{\text{uncat}}$ is decreased 28-fold with 14D9 and 12-fold with 20B11 and K_{TS} is increased 6- and 3.8-fold, respectively).

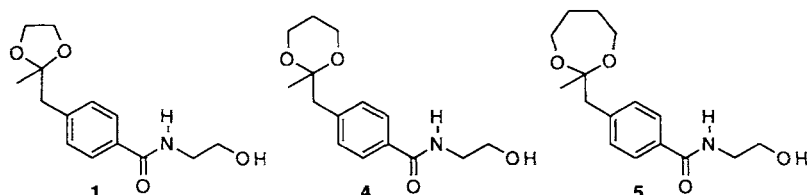
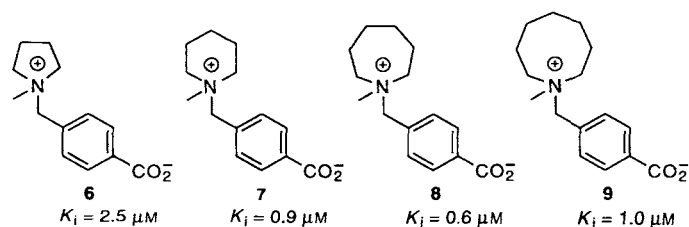


Table 1. Kinetic data for antibody-catalyzed hydrolysis of ketals **1**, **4**, and **5** (K_{m} and K_{TS} in μM).

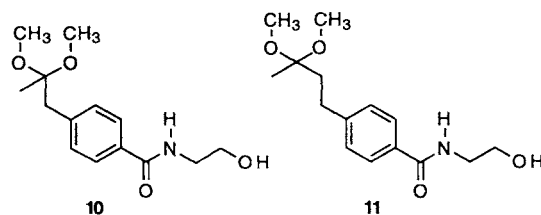
Anti-body	1			4			5		
	K_{m}	$k_{\text{cat}}/k_{\text{uncat}}$	K_{TS}	K_{m}	$k_{\text{cat}}/k_{\text{uncat}}$	K_{TS}	K_{m}	$k_{\text{cat}}/k_{\text{uncat}}$	K_{TS}
14D9	143	113	1.3	250	43	5.8	30	4	7.8
20B11	1095	870	1.3	403	106	3.8	376	76	5.0

Antibody 14D9 was chosen for further studies because it showed a more distinct shape discrimination in catalysis. The shape complementarity between this antibody and the piperidinium ring was estimated by measuring competitive inhibitions with hapten homologs having larger rings. For convenient kinetic analysis with this series of inhibitors their binding efficiency was uniformly reduced by changing the 2-hydroxyethylamide side chain to a carboxylate functionality.^[12] Antibody 14D9 bound pyrrolidinium **6** ($K_{\text{i}} = 2.5 \mu\text{M}$)^[12] less tightly than piperi-



dinium **7** ($K_{\text{i}} = 0.9 \mu\text{M}$)^[12] and showed almost no discrimination between **7** and its two higher homologs, azepinium **8** ($K_{\text{i}} = 0.6 \mu\text{M}$) and the ion **9** ($K_{\text{i}} = 1.0 \mu\text{M}$).^[13]

The active site of antibody 14D9 has been shown previously to possess an ionizable functionality, presumably an aspartate or glutamate side chain, capable of general acid-base catalysis.^[14] The solvent kinetic isotope effect in the 14D9-catalyzed hydrolysis of **1** showed that the reaction is specific acid catalyzed ($k_{\text{catH}}/k_{\text{catD}} = 0.4$), with no direct participation of this protein side chain as a general acid. In this case the antibody side chain might act as an electrostatic point charge that stabilizes the transition state.^[15] Substrate **4** ($K_{\text{m}} = 250 \mu\text{M}$), which can be considered as a neutral analog of the hapten, was bound by antibody 14D9 approximately 10^4 -fold less tightly than the hapten **3b** ($K_{\text{i}} \approx 10^{-8} \text{M}$). In fact the actual transition states for hydrolysis of **1**, **4**, and **5**, whose affinities are given by K_{TS} , are bound approximately 10^2 times tighter than the substrates themselves. These effects on transition state and hapten binding are much stronger than those seen by modulating molecular shapes and indicate that catalysis of ketal hydrolysis with antibody 14D9 depends primarily on electrostatic complementarity. This is also consistent with the observation that dimethyl ketal **10** ($k_{\text{cat}}/k_{\text{uncat}} = 70$, $K_{\text{m}} = 70 \mu\text{M}$) and its homolog **11** ($k_{\text{cat}}/k_{\text{uncat}} = 430$, $K_{\text{m}} = 230 \mu\text{M}$)^[16] are also substrates of antibody 14D9.^[17] The substrate's shape probably plays only a limited role in enabling the formation of a catalytically productive complex with the antibody.



We have shown here that antibodies catalyzing the hydrolysis of unactivated ketals can be achieved by a very simple design. We have presented evidence that the observed catalysis is triggered by electrostatic complementarity of the antibody binding site to the transition state, and that the effect of shape complementarity on catalysis is relatively limited. Since the hydrolysis of unactivated ketals is mechanistically closely related to the cleavage of glycosidic bonds, this study provides experimental support for the hypothesis that glycosidases would have first appeared as "electrostatic" catalysts. Shape complementarity and general acid catalysis, which dominate the catalytic effect in modern glycosidase,^[3] would only have emerged in the later course of evolution.

Received: June 20, 1996 [Z92471E]
German version: *Angew. Chem.* 1996, 108, 2800–2802

Keywords: catalytic antibodies · enzyme models · ketals

- [1] P. G. Schultz, R. A. Lerner, *Science* 1995, 269, 1835.
- [2] P. A. Patten, N. S. Gray, P. L. Yang, C. B. Marks, G. J. Wedemayer, J. J. Boniface, R. C. Stevens, P. G. Schultz, *Science* 1996, 271, 1086.
- [3] a) A. J. Kirby, *CRC Crit. Rev. Biochem.* 1987, 22, 283; b) M. L. Sinnott, *Chem. Rev.* 1990, 90, 1171; c) P. Deslongchamps, *Stereoelectronic Effects in Organic Chemistry (Organic Chemistry Series, Vol. 1)* (Ed.: J. E. Baldwin), Pergamon, Oxford, 1989.
- [4] A commonly accepted argument to explain this catalysis is the existence of strain. Binding by the enzyme induces strain in the glycoside substrate to a point where it becomes sensitive to catalysis by carboxylic acids. See [3].

- [5] a) T. H. Fife, S. H. Jaffe, R. Natarajan, *J. Am. Chem. Soc.* **1991**, *113*, 7646; b) T. H. Fife, E. Anderson, *ibid.* **1971**, *93*, 6610.
- [6] a) J.-L. Reymond, K. D. Janda, R. A. Lerner, *Angew. Chem.* **1991**, *103*, 1690; *Angew. Chem. Int. Ed. Engl.* **1991**, *30*, 1711; b) J. Yu, L. C. Hsieh, L. Kochersperger, S. Yonkovich, J. S. Stephens, M. A. Gallop, P. G. Schultz, *ibid.* **1994**, *106*, 327 bzw. **1994**, *33*, 339.
- [7] E. Anderson, T. H. Fife, *J. Am. Chem. Soc.* **1969**, *91*, 7163.
- [8] All ketals were prepared from methyl (4-bromomethyl)benzoate in a four-step sequence: Cross-coupling with divinyl cuprate [prepared from vinylmagnesium bromide (2 equiv) and cuprous iodide (1 equiv) in THF at -30°C] afforded methyl (4-allyl)benzoate. Wacker oxidation at room temperature with PdCl_2 (0.1 equiv) and CuCl_2 (1.5 equiv) in $\text{DMF}/\text{H}_2\text{O}$ (2/1) afforded (4-methoxycarbonyl)phenylacetone, which was ketalized in benzene at reflux in the presence of the appropriate diol (ethylene glycol, 1,3-dihydroxypropane, 1,4-dihydroxybutane) and catalytic amounts of *p*-toluenesulfonic acid. Dimethyl ketal **10** was obtained by treating the corresponding ketone with trimethylorthoformate and methanol in the presence of *p*-toluenesulfonic acid. Finally, the methyl ester was converted to the 2-hydroxyethylamide by heating it in 2-aminoethanol (100°C , 2 h).
- [9] A. Koch, J.-L. Reymond, R. A. Lerner, *J. Am. Chem. Soc.* **1994**, *116*, 803.
- [10] All reactions were carried out at 24°C with $5\ \mu\text{M}$ antibody and $50\text{--}2000\ \mu\text{M}$ substrate in 1,3-bis[tris(hydroxymethyl)methylamino]propane-buffered saline solution (50 mM buffer, 50 mM NaCl, pH 6.0). The progress of the reaction was monitored by HPLC (Hitachi L-6200A; $\lambda = 254\ \text{nm}$; C18-RP column (25 cm \times 2.2 mm, $5\ \mu\text{m}$), eluting with 20% acetonitrile in water (retention times in minutes: **2**: 5.2, **1**: 9.83, **4**: 9.95, **5**: 23.06).
- [11] a) B. Ganem, G. Papandreou, *J. Am. Chem. Soc.* **1991**, *113*, 8984; b) H. Suga, N. Tanimoto, A. J. Sinskey, S. Masamune, *ibid.* **1994**, *116*, 11197.
- [12] G. K. Jahangiri, J.-L. Reymond, *J. Am. Chem. Soc.* **1994**, *116*, 11264.
- [13] Compounds **8** and **9** were prepared by alkylation of hexamethylene imine and heptamethylene imine, respectively, with methyl (4-bromomethyl) benzoate, followed by quaternization with iodomethane and saponification with aqueous NaOH. The products were purified by preparative RP-HPLC (water/acetonitrile gradient) and obtained as trifluoroacetate salts (colorless solids). Competitive inhibition constants of **8** and **9** were measured following the procedure described for **6** and **7** [12].
- [14] a) J.-L. Reymond, G. K. Jahangiri, C. Stoudt, R. A. Lerner, *J. Am. Chem. Soc.* **1993**, *115*, 3909; b) S. C. Sinha, E. Keinan, J.-L. Reymond, *ibid.* **1993**, *115*, 4893; c) D. Shabat, H. Itzaky, J.-L. Reymond, E. Keinan, *Nature* **1995**, *374*, 143.
- [15] Antibody 14D9 has been cloned and its sequence shows five aspartate or glutamate residues in the CDR regions. J.-L. Reymond, C. F. Barbas, unpublished results.
- [16] S. C. Sinha, E. Keinan, J.-L. Reymond, *Proc. Natl. Acad. Sci. USA* **1993**, *90*, 11910.
- [17] Hydrolysis of **10** was carried out at 24°C , pH 7.4, and that of **11** at 0°C , pH 7.55; both were conducted in 50 mM phosphate/100 mM NaCl).

Synthesis and Structure of $\text{CoB}_2\text{P}_3\text{O}_{12}(\text{OH})\cdot\text{C}_2\text{H}_{10}\text{N}_2$: The First Metal Borophosphate with an Open Framework Structure**

Slavi C. Sevov*

The most notable trend in the field of molecular sieve synthesis in the past few years is the profound expansion of the variety of studied systems and the rapidly growing number of acronyms associated with them. In addition to the conventional zeolites there are AlPOs (Al-P-O systems), SAPOs (Si-Al-P-O systems), GaPOs (Ga-P-O systems), MeAPOs (metal-Al-P-O systems), Ga-As-O systems, Al-As-O systems, etc. Virtually all combina-

tions of the mixed oxides of the heavier analogs of the boron and nitrogen groups have been explored. With this in mind it is quite surprising that molecular sieves in the B-P-O or Me-B-P-O systems have not yet been synthesized. This is even more surprising considering that BPO_4 itself is a catalyst used industrially for many reactions including hydration, dehydration, alkylation, and oligomerization,^[1] and extensive research efforts have been devoted to finding ways to increase its surface-to-volume ratio.^[2] Furthermore, incorporation of boron in zeolites and molecular sieves has been a goal pursued for quite some time, since even small amounts of boron have been shown to improve enormously the properties of the host.^[3] With a few exceptions, however,^[4] such boron incorporation has been possible only on a very small scale, usually less than one percent.^[3a, 5] Reported here is the first member of a new class of molecular sieves, namely metal borophosphates (BPOs) with open framework structures in which boron is an integral part of the framework.

The title compound (designated BPO-1) was made hydrothermally from H_3BO_3 , H_3PO_4 , $[\text{Co}(\text{en})_3\text{Cl}_3]$ (en = ethylenediamine), and $\text{BF}_3\cdot\text{CH}_3\text{CH}_2\text{NH}_2$. Although fluorine is not incorporated in the compound (see Experimental Procedure), boron trifluoride apparently plays an important role in the synthesis since attempts to make the compound without it or with other fluoride sources were unsuccessful. The role of fluorides in the formation of novel framework structures has been well documented, although it is not quite clear what exactly that role might be.^[6]

The structure of BPO-1 was determined by single-crystal X-ray diffraction (see Experimental Procedure). The atomic coordinates and some selected bond lengths are listed in Tables 1 and 2, respectively. The structure of the deep purple BPO-1 can be best described as an open framework with one-dimensional channels along the *b* direction of the orthorhombic unit cell (Fig. 1). The framework is built of corner-sharing CoO_6 octahedra and BO_4 and PO_4 tetrahedra. All but two oxygen atoms are shared by two polyhedra. The two exceptions are O13, which is shared by three polyhedra (one CoO_6 octahedron and two BO_4 tetrahedra), and O12, which belongs to only one polyhedron (PO_4 tetrahedron) and is a part of an OH group. No two

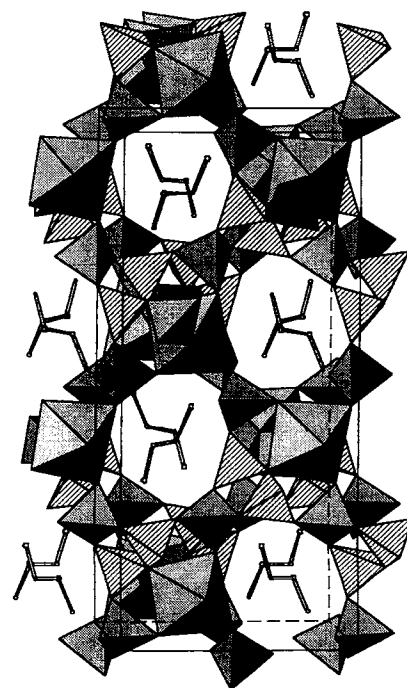


Fig. 1. View of BPO-1 nearly along the *b* axis; the *c*-axis is vertical and the unit cell is outlined. The striped tetrahedra are BO_4 units and the rest are PO_4 units. The octahedra correspond to CoO_6 . The ethylenediamine molecules are shown without the hydrogen atoms.

[*] Prof. S. C. Sevov
Department of Chemistry and Biochemistry
University of Notre Dame
Notre Dame, IN 46556 (USA)
Fax: Int. code + (219) 631-6652
e-mail: ssevov@nd.edu

[**] I thank Dr. A. G. Lappin for his suggestions and Dr. M. Shang for his help with X-ray data collection.